Available online at www.sciencedirect.com

ScienceDirect

Journal of Non-Crystalline Solids 354 (2008) 2435–2439

JOURNAL OF NON-CRYSTALLINE SOLIDS

www.elsevier.com/locate/jnoncrysol

Advanced deposition phase diagrams for guiding Si:H-based multijunction solar cells

J.A. Stoke [a], N.J. Podraza [a,b], Jian Li [a], Xinmin Cao [a], Xunming Deng [a], R.W. Collins [a,*]

[a] *Department of Physics and Astronomy, University of Toledo, Toledo, OH 43606, USA*

[b] *Materials Research Institute, The Pennsylvania State University, University Park, PA 16803, USA*

Available online 4 February 2008

Abstract

Phase diagrams have been established to describe very high frequency (vhf) plasma-enhanced chemical vapor deposition (PECVD) of intrinsic hydrogenated silicon (Si:H) and silicon–germanium alloy ($Si_{1-x}Ge_x$:H) thin films on crystalline Si substrates that have been over-deposited with n-type amorphous Si:H (a-Si:H). The Si:H and $Si_{1-x}Ge_x$:H films are prepared under conditions used for the top and middle i-layers of high efficiency triple-junction a-Si:H-based n–i–p solar cells. Identical n/i cell structures were co-deposited in this study on textured (stainless steel)/Ag/ZnO which serve as substrate/back-reflectors in order to relate the phase diagrams to the performance parameters of single-junction solar cells. This study has reaffirmed that the highest efficiencies for a-Si:H and a-$Si_{1-x}Ge_x$:H solar cells are obtained when the i-layers are prepared under previously-described maximal H_2 dilution conditions.
Published by Elsevier B.V.

PACS: 07.60.Fs; 84.60.Jt; 81.15.Gh

Keywords: Silicon; Solar cells; Optical spectroscopy

1. Introduction

State-of-the-art solar cells based on a-Si:H prepared by PECVD employ a triple-junction design [1,2]. Optimization of the a-Si:H i-layer of the top cell has been widely successful through the maximal H_2 dilution concept [3,4]. This entails operating the PECVD process at the highest H_2 dilution while avoiding the tendency of the film to evolve to a mixed-phase amorphous + microcrystalline structure with increasing thickness. The benefits of H_2 dilution include enhanced surface passivation and hence diffusion of film precursors in the PECVD process, as well as enhanced relaxation of sub-surface strained Si–Si bonds [4]. The resulting 'protocrystalline' nature of the i-layer prepared with maximal H_2 dilution provides the highest device performance and stability. In this study, vhf PECVD phase diagrams have been developed for Si:H and $Si_{1-x}Ge_x$:H i-layers deposited from $Si_2H_6 + GeH_4$ mixtures on a-Si:H n-layers under the conditions used for high-efficiency triple-junction n–i–p cells. These diagrams have been correlated with single-junction cell performance in order to further explore applicability of the maximal H_2 dilution concept for the highest quality $Si_{1-x}Ge_x$:H i-layers.

2. Experimental details

The Si:H and $Si_{1-x}Ge_x$:H i-layers for phase diagram development by real time spectroscopic ellipsometry (RTSE) were deposited on c-Si/(native-oxide)/(n-type a-Si:H) substrate structures using multichamber vhf (70 MHz) PECVD. Such substrates ensure a specular surface to aid in the utilization of RTSE with the highest possible sensitivity. This is the first such study that directly correlates PECVD phase diagrams for a-$Si_{1-x}Ge_x$:H i-layers with the performance of solar cells incorporating these i-layers. In order to establish these correlations for insights into n–i–p cell performance, additional samples ~2000 Å

* Corresponding author.
E-mail address: robert.collins@utoledo.edu (R.W. Collins).

0022-3093/$ - see front matter Published by Elsevier B.V.
doi:10.1016/j.jnoncrysol.2007.10.061

thick were co-deposited onto textured (stainless steel)/Ag/ZnO/(n-type a-Si:H) structures in the device configuration simultaneously with the specular c-Si/(native-oxide)/(n-type a-Si:H) substrates. For depositions performed versus the phase diagram variable $R = [H_2]/\{[Si_2H_6] + [GeH_4]\}$, all other parameters were selected as those used for the previously-optimized top and middle i-layers of a triple junction solar cell. These parameters include a vhf power of 8 W, a low source gas $[Si_2H_6] + [GeH_4]$ partial pressure of $p < 0.004$ Torr, a total gas pressure of $p_{tot} \sim 0.2$ Torr, and nominal substrate temperatures of $T = 200$ °C for Si:H and $T = 350$ °C for $Si_{1-x}Ge_x$:H. These nominal temperatures actually correspond to calibrated values of $T = 107$ °C and 170°C, respectively, determined by RTSE [5]. The flow ratio $G = [GeH_4]/\{[Si_2H_6] + [GeH_4]\}$ was set at 0 for the top i-layer, resulting in growth rates ranging from ~2.3 to ~0.8 Å/s as R increases from 60 to 150. For the middle i-layer G was set to 0.286, resulting in growth rates ranging from ~2.6 to ~1.1 Å/s as R increases from 45 to 150.

Analysis of RTSE data obtained using a rotating-compensator multichannel instrument [6] enables the determination of the complex dielectric function ε of the growing film as well as the evolution of the bulk layer thickness $d_b(t)$ and surface roughness layer thicknesses $d_s(t)$. From $d_b(t)$, the instantaneous deposition rate $r(t)$ can be determined. For films whose phase and optical properties are evolving continuously with thickness, a virtual interface RTSE analysis technique is applied that yields the near surface dielectric function continuously with time $\varepsilon(t)$, as well as $r(t)$ and $d_s(t)$. By integrating $r(t)$, a depth profile in the dielectric function $\varepsilon(d_b)$ can be established which in turn can be interpreted via effective medium theory to extract a depth profile in the microcrystalline volume fraction $f_{\mu c}(d_b)$.

3. Results

Fig. 1(a) shows typical results for surface roughness layer thickness versus bulk layer thickness during Si:H growth with two H_2 dilution levels. Examples are provided for a Si:H film that remains amorphous throughout growth ($R = 60$) and for one in which microcrystallites nucleate from the amorphous phase, grow preferentially, and ultimately coalesce to a single-phase microcrystalline structure ($R = 150$). In particular, the $R = 150$ data reveal the amorphous-to-(mixed-phase microcrystalline) roughening transition, denoted a → (a + μc), and the (mixed-phase)-to-(single-phase) microcrystalline smoothening transition, denoted (a + μc) → μc. The RTSE data for such a film can be analyzed using the virtual interface technique designed in this case to extract the dielectric function of the top ~10 Å of the bulk layer as well as the instantaneous deposition rate and thus to generate a depth profile in the microcrystalline fraction $f_{\mu c}(d_b)$ as shown in Fig. 1(b).

Similar depth profiles $f_{\mu c}(d_b)$ were compiled for Si:H films prepared versus R in order to establish the contours

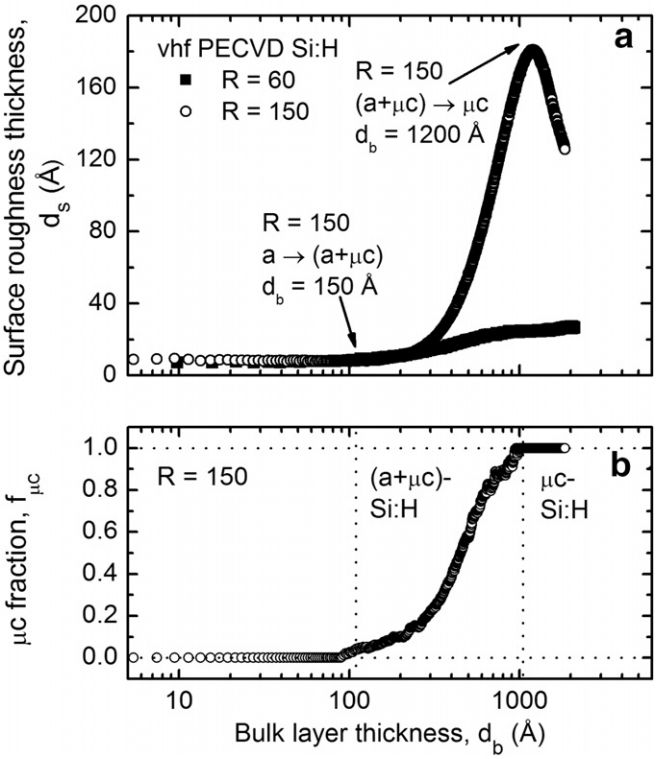

Fig. 1. (a) Surface roughness evolution for vhf PECVD Si:H films in the fully amorphous growth regime ($R = 60$) and in the microcrystalline evolution regime ($R = 150$); (b) the microcrystallite volume fraction in the top 10 Å of the bulk layer plotted versus the accumulated bulk layer thickness for the $R = 150$ Si:H film, as determined from RTSE analysis.

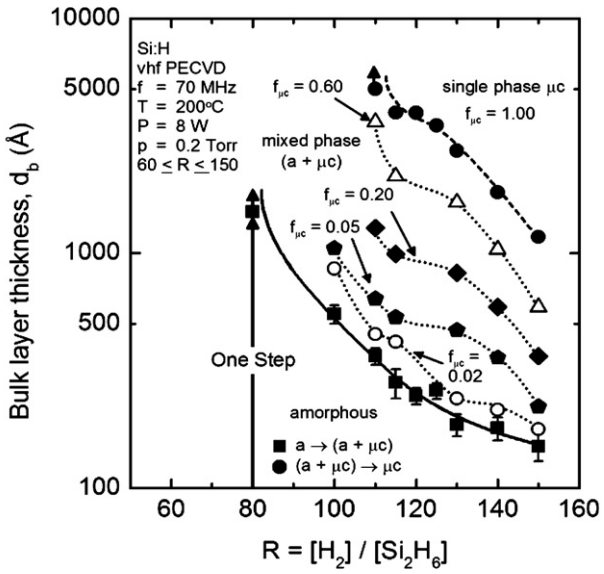

Fig. 2. A deposition phase diagram for vhf PECVD Si:H with $G = [GeH_4]/\{[Si_2H_6] + [GeH_4]\} = 0$ including the a → (a + μc) transition (solid line, squares) and the (a + μc) → μc transition (dashed line, circles) thicknesses, as deduced from data such as those of Fig. 1. Up-arrows indicate that the transitions occur at thicknesses above the indicated values. Contour lines in the crystallite volume fraction $f_{\mu c}$ are also plotted.

of the phase diagram in Fig. 2. This diagram demonstrates that, under the vhf PECVD conditions used here, the Si:H

films remain amorphous throughout at least ~2000 Å of bulk layer growth for $R \leqslant 80$. At higher H_2 dilution ($100 \leqslant R \leqslant 150$), the Si:H films initially nucleate as a-Si:H but undergo the a → (a + μc) transition at a thickness that decreases with increasing R. Fig. 2 shows that the surface roughening onset (shown in the data for $R = 150$ in Fig. 1), which identifies the nominal a → (a + μc) transition given by the solid line in Fig. 2, provides sensitivity to this transition at a microcrystalline volume fraction of less than 0.02 within the near-surface of the bulk layer.

The structural and phase evolution of the $Si_{1-x}Ge_x$:H exhibits behavior analogous to that of the Si:H series. The surface roughness and microcrystallite evolution data acquired for depositions at varying R were used to compile the vhf PECVD phase diagram in Fig. 3. This diagram demonstrates that the $Si_{1-x}Ge_x$:H films remain amorphous throughout ~2000 Å of bulk layer growth for $R \leqslant 70$. At higher H_2 dilutions ($80 \leqslant R \leqslant 150$), the films initially nucleate on the underlying n-layer as a-$Si_{1-x}Ge_x$:H but, as in the case of Si:H, undergo the a → (a + μc) transition at a thickness that decreases with increasing R. Fig. 3 shows that although the a → (a + μc) transition obtained directly from the roughening onset (solid line) is sensitive to microcrystalline volume fractions of <0.02 in the near-surface of the bulk layer at low R, the sensitivity degrades at higher R as the a → (a + μc) transition shifts to lower thickness.

The n–i structures co-deposited on the textured ss/Ag/ZnO stacks (serving as the substrate/back-reflector) from the two series of Figs. 1–3 (including additional films in which the depositions were terminated at the device i-layer thickness of ~2000 Å) were then fabricated into single-junction solar cells with 25 °C Tauc gaps of ~1.8 eV and ~1.5 eV for the top and middle i-layers, respectively. The cells were characterized to extract the open circuit voltage

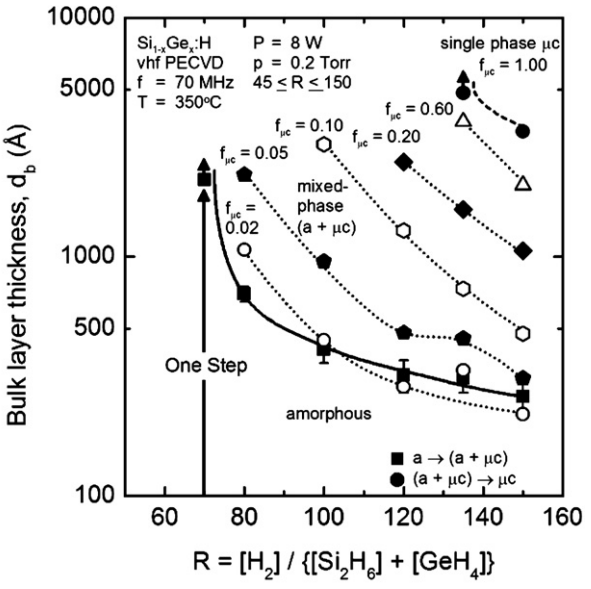

Fig. 3. A deposition phase diagram for vhf PECVD $Si_{1-x}Ge_x$:H with $G = 0.286$ analogous to that of Fig. 2 for Si:H.

(V_{oc}), short circuit current (J_{sc}), fill factor (FF), and efficiency (η). Results for a-Si:H with $G = [GeH_4]/\{[Si_2H_6] + [GeH_4]\} = 0$, and for the alloys with $G = 0.286$ are given in Figs. 4 and 5, respectively, and will be discussed in detail in Section 4.

4. Discussion

The phase diagrams for vhf PECVD from $Si_2H_6 + GeH_4$ of Figs. 2 and 3 show features characteristic of previous diagrams for films from $SiH_4 + GeH_4$. Thus, by understanding the nature of microcrystallite evolution and quantifying the phase composition as in Figs. 2 and 3, it may be possible to select H_2 dilution levels in order to maximize film quality for one-step, multi-step, or graded layers.

In the case of a 2000 Å thick a-Si:H i-layer, the optimum one-step deposition process is predicted on the basis of the phase diagram to occur at the maximal value of $R = 80$, i.e., the largest R possible such that the i-layer remains amorphous throughout its thickness during growth. This prediction is borne out in the device performance of Fig. 4. At $R = 100$ the a → (a + μc) transition occurs at 600 Å, however, and the Si:H microcrystallite fraction in the near-surface of the 2000 Å i-layer is ~0.09. These crystallites appear to degrade V_{oc} significantly due to their presence at the i/p interface. The one-step optimized process for a 2000 Å thick a-$Si_{1-x}Ge_x$:H i-layer is expected at $R = 70$ according to the same principle, and this optimum is also borne out in the device performance of Fig. 5, but much less distinctly. Above $R = 70$ a detectable volume fraction of microcrystalline $Si_{1-x}Ge_x$:H is present in the near-surface of the film ranging from 0.05 at $R = 80$ to 0.08 at $R = 100$. In contrast to Si:H, the presence of the microcrystallites at the i/p interface of the $Si_{1-x}Ge_x$:H solar cells does not significantly decrease V_{oc} and efficiency. Although the overall performance of the devices remains acceptable for $70 < R \leqslant 100$ in Fig. 5, this region is avoided due to irreproducibility, including a strong dependence on the underlying n-layer structure and poor yield. Next V_{oc} and FF will be discussed further with possible strategies for future multistep improvements.

Considering first the variation in V_{oc} for Si:H in Fig. 4, this parameter increases with increasing R for i-layers below the optimum at $R = 80$ due to the increase in band gap; however, a more abrupt increase occurs that defines the optimum as the a → (a + μc) transition is approached. This is the protocrystalline regime, characterized by an improvement in ordering as well as an increase in gap. Because V_{oc} is strongly influenced by the film properties at the very top of the i-layer near the i/p interface, there is an abrupt decrease in its value above $R = 80$ due to the presence of crystalline nuclei at the top of the film. When the top of the film is mixed-phase Si:H, V_{oc} lies between the values for protocrystalline Si (~1 eV) and μc-Si:H (~0.5 eV). For R values above the (a + μc) → μc

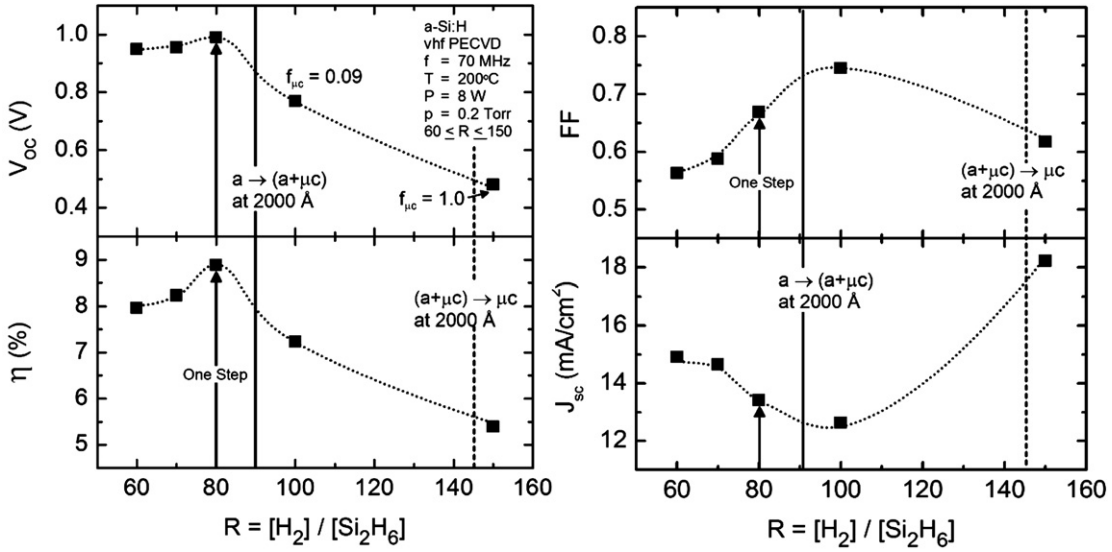

Fig. 4. Open circuit voltage (V_{oc}, upper left), efficiency (η, lower left), fill factor (FF, upper right), and short circuit current (J_{sc}, lower right) versus R of the i-layer for vhf PECVD Si:H solar cells.

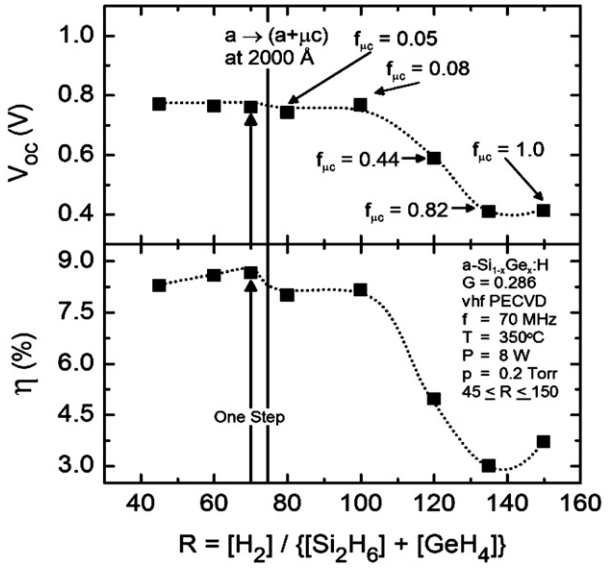

Fig. 5. Open circuit voltage (V_{oc}, upper) and efficiency (η, lower) versus R of the i-layer for vhf PECVD $Si_{1-x}Ge_x$:H solar cells.

transition for a 2000 Å thick film, a V_{oc} value appropriate for μc-Si:H is expected.

In contrast, V_{oc} for $Si_{1-x}Ge_x$:H in Fig. 5 shows only a weak dependence on R throughout the amorphous growth regime and even across the a → (a + μc) transition. In this case, the effect of R on the optical band gap of $Si_{1-x}Ge_x$:H is also weaker. The lack of a strong effect of the i/p interface crystallites for $Si_{1-x}Ge_x$:H may be due to the fact that over a wide range of R the microcrystallites do not appear to grow preferentially as cone-like structures as in Si:H, but rather as isolated nanoclusters.

The behavior of the fill factor (FF) with R for both Si:H and $Si_{1-x}Ge_x$:H suggests the possibility of an improvement in the cell performance with multistep processing. As an example, Fig. 4 shows that, although the FF increases with R, its maximum of 0.74 is reached at an R value larger than that which maximizes V_{oc}. Because the FF is controlled predominantly by the bulk i-layer, the presence of crystallites that evolve to a small volume fraction in the upper portion of the film, protrude at the i/p interface, and reduce V_{oc}, however, does not adversely affect the FF. The FF actually seems to benefit from the incorporation of microcrystallites in the bulk of the Si:H. This improvement may in fact be due to an improvement in the properties of the amorphous component of the mixed phase material (i.e., increases in the band gap and protocrystalline ordering) when it is deposited with increasing R from 80 to 100. One may be able to take advantage of an optimum V_{oc} and FF simultaneously by depositing the bulk (~1800 Å) of the i-layer with $R = 100$, then depositing a thin (<100 Å) substrate-memory-erasing low R layer – similar to the starting n-layer, before finally completing the cell with a second ~200 Å $R = 100$–120 layer. The key, however, is to ensure that the memory-erasing layer first is successful at suppressing the continued growth of crystallites, and second is not detrimental to the FF.

5. Summary

Deposition phase diagrams have been developed and augmented for vhf PECVD of thin film Si:H and its alloys with Ge by including contour lines that represent the crystalline volume fraction in the top ~10 Å of the i-layer at a given bulk layer thickness. These diagrams predict optimum one-step i-layer deposition processes for the top and middle cells of a triple-junction device that are in consistency with the performance of single-junction devices. V_{oc} and FF appear to be optimized at different values of

R suggesting that a multistep vhf PECVD process may be beneficial.

Acknowledgement

This research was supported by the National Renewable Energy Laboratory (Subcontract No. RXL-5-44205-06).

References

[1] J. Yang, A. Banerjee, S. Guha, Appl. Phys. Lett. 70 (1997) 2975.
[2] X. Deng, X.B. Liao, S.J. Han, H. Povolny, P. Agarwal, Sol. Energy Mater. Sol. Cells 62 (2000) 89.
[3] D.V. Tsu, B.S. Chao, S.R. Ovshinsky, S. Guha, J. Yang, Appl. Phys. Lett. 71 (1997) 1317.
[4] R.W. Collins, A.S. Ferlauto, Curr. Opin. Solid State Mater. Sci. 6 (2002) 425.
[5] P. Lautenschlager, M. Garriga, L. Viña, M. Cardona, Phys. Rev. B 36 (1987) 4821.
[6] I. An, J.A. Zapien, C. Chen, A.S. Ferlauto, A.S. Lawrence, R.W. Collins, Thin Solid Films 455 (2004) 132.